A Comparison Study of Some Configurations of the Uninorm Morphological Edge Detector

Manuel González-Hidalgo, Sebastià Massanet, Arnau Mir and Daniel Ruiz-Aguilera

Dept. of Mathematics and Computer Science, University of the Balearic Islands, Crta. Valldemossa Km. 7.5, Palma, Spain

Abstract: In this paper, we study the performance of the edge detector from the fuzzy mathematical morphology based on conjunctive uninorms. Several different pairs of uninorm and fuzzy implication (configurations) are considered in the fuzzy morphological gradient. The results are compared using an objective edge detection performance measure, the so-called Pratt's figure of merit. To reinforce the analysis a K-means clustering algorithm has been applied to study the relation between the configurations and to determine which uninorm and implication have to be chosen to obtain an optimal edge detector. According to the analysis of the obtained results, the idempotent uninorm obtained using the classical negation, and its residual implication is the best configuration in this framework.

1 INTRODUCTION

Edge detection is a fundamental low-level operation in image processing, that is essential to develop high-level operations such as segmentation, computer vision and recognition. Its performance is crucial for the final results of the image processing technique. In recent decades, a large number of edge detection algorithms have been developed. These different approaches vary from classical algorithms (Pratt, 2007) based on the use of a set of convolution masks, to new techniques based on fuzzy sets and their extensions (Bustince et al., 2009).

Among the fuzzy approaches, we can highlight the fuzzy mathematical morphology that generalizes the binary morphology (Serra, 1988) using concepts and techniques of the fuzzy set theory (see (Bloch and Maître, 1995), (Nachtegael and Kerre, 2000)). This theory allows a better treatment and a more flexible representation of the uncertainty and ambiguity present in every level of an image. Morphological operators are the basic tools of this theory. A morphological operator P transforms an image A to be analysed in a new image $P(A, B)$ by means of an structuring element B. The four basic morphological operations are dilation, erosion, opening and closing. Since gray-level images can be represented as fuzzy sets, fuzzy tools can be used to define fuzzy morphological operators. This approach was introduced by De Baets in (De Baets, 1997) and (De Baets, 2000) esta-

blishing a general framework where fuzzy morphological operators are defined using conjunctions and fuzzy implications. The first step was based on the use of t-norms in $[0, 1]$ as conjunctions and their residual implications as fuzzy implications. After analysing which properties must satisfy the t-norm and the implication to generate a fuzzy mathematical morphology with all the desirable algebraical properties, it was concluded that the couple formed by a nilpotent t-norm and its residual implication generates a "good" fuzzy mathematical morphology. Since nilpotent t-norms are conjugates of the Łukasiewicz t-norm T_{LK}, this t-norm and its residual implication, that is the Łukasiewicz implication I_{LK}, are usually chosen to define the fuzzy morphological operators of this theory. Recently, it has been introduced a fuzzy mathematical morphology based on discrete t-norms with good results in applications (González-Hidalgo et al., 2010) using the fact that gray-level images are represented in fact as $\mathbb{Z}^2 \to L$ functions, where L is a finite chain containing the gray-level values and not as $\mathbb{R}^2 \to [0, 1]$ functions.

However, other classes of conjunctions have been used. In particular, the use of conjunctive uninorms and their residual implications have been recently proposed leading to a new fuzzy morphology that improves the results in some applications, specially in edge detection and noise removal (González-Hidalgo et al., 2009b).

Focusing on edge detection purposes, the fuzzy

morphology must satisfy the extensivity and the anti-extensivity of the erosion. This is the key property for defining an edge detector based on the fuzzy morphological gradient. Taking into account that the pair (T_{LK}, I_{LK}) is the representative of the configurations which define fuzzy morphological operators satisfying all the desirable algebraical properties, this configuration has been widely used to implement the edge detector of the fuzzy morphology based on t-norms.

However, the mentioned property is satisfied with some minimal properties of the structuring element, the t-norm and the implication. Thus in (González-Hidalgo et al., 2012) many more t-norms and implications were used to define a morphological gradient useful to detect edges. There, it was proved that the pair (T_{LK}, I_{LK}) was the worst of the 40 considered configurations, while (T_{nM}, I_{KD}), where

$$T_{nM}(x,y) = \begin{cases} 0 & \text{if } x + y \leq 1, \\ \min\{x, y\} & \text{otherwise,} \end{cases}$$

and $I_{KD}(x,y) = \max\{1 - x, y\}$, was the best configuration generating a notable edge detector.

The aim of this contribution is to perform a similar study for the fuzzy morphology based on conjunctive uninorms. Only some particular uninorms with their residual implications have been considered in the fuzzy morphological gradient of this approach, but similarly to the case of t-norms, many more uninorms and fuzzy implications can be chosen to generate the gradient. Thus we want to determine the best combination of uninorm and implication to define an optimal edge detector in this morphology. The results will be objectively compared using Pratt's figure of merit, *FoM* (Pratt, 2007). To compute this measure, the edge image must be binarized and thinned to obtain edges with one-pixel width. This conditions are consistent with Canny's restrictions, set out in (Canny, 1986). Therefore, after obtaining the fuzzy edge image using the fuzzy gradient, this image is thinned using *Non-Maxima Suppression* (NMS), a well-known thinning algorithm proposed by Canny, and the recently introduced automatic hysteresis algorithm based on determining a "zone of instability" in the histogram proposed in (Medina-Carnicer et al., 2011) to binarize the image.

The communication is organized as follows. In Section 2, we recall the definitions of morphological operators and fuzzy operators that define them. In Section 3, we present the considered uninorms and implications, and the algorithm developed for each configuration. In the next section, the results are presented and analysed. Finally, we share the conclusions and future work we want to develop.

2 PRELIMINARIES

Fuzzy morphological operators are defined using fuzzy operators such as uninorms and implications. More details on these logical connectives can be found in (Fodor et al., 1997) and (Baczyński and Jayaram, 2008), respectively.

Definition 1. A *uninorm* is a commutative, associative, non-decreasing function $U : [0,1]^2 \to [0,1]$ with neutral element $e \in (0,1)$, i.e., $U(e,x) = U(x,e) = x$ for all $x \in [0,1]$.

A uninorm U such that $U(0,1) = 0$ is called *conjunctive* and if $U(0,1) = 1$, then it is called *disjunctive*.

Definition 2. A binary operator $I : [0,1]^2 \to [0,1]$ is a *fuzzy implication* if it is decreasing in the first variable, increasing in the second one and it satisfies $I(0,0) = I(1,1) = 1$ and $I(1,0) = 0$.

Thus, we can define the basic fuzzy morphological operators such as dilation and erosion. From now on, we will use the following notation: U denotes a conjunctive uninorm, I an implication, A a gray-level image, and B a gray-level structuring element.

Definition 3. The *fuzzy dilation* $D_U(A,B)$ and the *fuzzy erosion* $E_I(A,B)$ of A by B are the gray-level images defined by

$$\begin{aligned} D_U(A,B)(y) &= \sup_x U(B(x-y), A(x)) \\ E_I(A,B)(y) &= \inf_x I(B(x-y), A(x)). \end{aligned}$$

As we have already mentioned, the following proposition ensures the extensivity of the fuzzy dilation and the anti-extensivity of the fuzzy erosion with some minimal properties.

Proposition 1. *Let U be a conjunctive uninorm with neutral element $e \in (0,1)$, I an implication that satisfies (NP_e), i.e., $I(e,y) = y$ for all $y \in [0,1]$ and B a gray-level structuring element such that $B(0) = e$. Then the following inclusions hold:*

$$E_I(A,B) \subseteq A \subseteq D_U(A,B).$$

Thus, as in the case of classical morphology, the difference between the fuzzy dilation and the fuzzy erosion of a gray-level image, $D_U(A,B) \setminus E_I(A,B)$, known as *fuzzy gradient operator*, can be used in edge detection.

3 CONFIGURATIONS AND ALGORITHM

According to Proposition 1, any conjunctive uninorm with neutral element $e \in (0,1)$ and any implication that satisfies (NP_e) are adequate to define the

Table 1: Considered uninorms.

Formula	Class
$U_1(x,y) = \begin{cases} \min\{x,y\} & \text{if } y \leq 1-x, \\ \max\{x,y\} & \text{if } y > 1-x. \end{cases}$	Idempotent
$U_2(x,y) = \begin{cases} \frac{xy}{(1-x)(1-y)+xy} & \text{if } (x,y) \notin \{(0,1),(0,1)\}, \\ 0 & \text{otherwise.} \end{cases}$	Representable
$U_3(x,y) = \begin{cases} \max\{x+y-\frac{1}{2},0\} & \text{if } x,y \leq \frac{1}{2}, \\ \min\{x+y-\frac{1}{2},1\} & \text{if } x,y \geq \frac{1}{2}, \\ \min\{x,y\} & \text{otherwise.} \end{cases}$	$U_{\min}$
$U_4(x,y) = \begin{cases} 0 & \text{if } y \leq \frac{1}{2}-x, \\ 1 & \text{if } y \geq \frac{3}{2}-x, \\ \max\{x,y\} & x,y \geq \frac{1}{2} \text{ and } y < \frac{3}{2}-x, \\ \min\{x,y\} & \text{otherwise.} \end{cases}$	$U_{\min}$
$U_5(x,y) = \begin{cases} \max\{x,y\} & \text{if } x,y \geq \frac{1}{2}, \\ \min\{x,y\} & \text{otherwise.} \end{cases}$	$U_{\min}$
$U_6(x,y) = \begin{cases} \min\{x,y\} & \text{if } y \leq \sqrt{1-x^2}, \\ \max\{x,y\} & \text{if } y > \sqrt{1-x^2}. \end{cases}$	Idempotent

fuzzy gradient. Until now, in this uninorm approach, only two types of left-continuous conjunctive uninorms and their residual implications have been used. Specifically, they are defined as follows:

- *Representable uninorms*: Let $e \in (0,1)$ and let $h : [0,1] \to [-\infty,\infty]$ be a strictly increasing continuous function with $h(0) = -\infty$, $h(e) = 0$ and $h(1) = \infty$. Then $U_h(x,y) =$

$$= \begin{cases} h^{-1}(h(x)+h(y)) & \text{if } (x,y) \notin \{(1,0),(0,1)\}, \\ 0 & \text{otherwise,} \end{cases}$$

is a conjunctive representable uninorm with neutral element e, and its residual implication I_{U_h} is given by $I_{U_h}(x,y) =$

$$= \begin{cases} h^{-1}(h(y)-h(x)) & \text{if } (x,y) \notin \{(0,0),(1,1)\}, \\ 1 & \text{otherwise.} \end{cases}$$

- A specific type of *idempotent uninorms*. Let N be a strong negation. The function given by

$$U^N(x,y) = \begin{cases} \min\{x,y\} & \text{if } y \leq N(x), \\ \max\{x,y\} & \text{otherwise,} \end{cases}$$

is a conjunctive idempotent uninorm. Its residual implication is given by

$$I_{U^N}(x,y) = \begin{cases} \min\{N(x),y\} & \text{if } y < x, \\ \max\{N(x),y\} & \text{if } y \geq x. \end{cases}$$

These two types of conjunctive uninorms guarantee most of the good algebraic and morphological properties associated with the morphological operators obtained from them (see (González-Hidalgo et al., 2009a)). Note that from these conjunctive uninorms, their residual implications satisfy (NP$_e$) since

any RU-implication[1] generated from a uninorm satisfies (NP$_e$) (see Proposition 5.4.2 in (Baczyński and Jayaram, 2008)). However, this property is not rare among the types of implications derived from uninorms, in fact it is also satisfied by the recently introduced (h,e)-implications as proves Proposition 9 in (Massanet and Torrens, 2011). This class of implications is generated by a continuous and strictly increasing function $h : [0,1] \to [-\infty,\infty]$ with $h(0) = -\infty$, $h(e) = 0$ and $h(1) = \infty$ as follows:

$$I^{h,e}(x,y) = \begin{cases} 1 & \text{if } x = 0, \\ h^{-1}\left(\frac{x}{e} \cdot h(y)\right) & \text{if } x > 0 \text{ and } y \leq e, \\ h^{-1}\left(\frac{e}{x} \cdot h(y)\right) & \text{if } x > 0 \text{ and } y > e. \end{cases}$$

Consequently, we have considered the conjunctive uninorms collected in Table 1 and the implications in Table 2. Six uninorms have been considered. U_1 and U_6 are the idempotent uninorms U^{N_C} where $N_C(x) = 1 - x$ for all $x \in [0,1]$ and U^{N^2}, where $N^2(x) = \sqrt{1-x^2}$, respectively. Moreover, U_2 is the representable uninorm U_h with $h(x) = \ln\left(\frac{x}{1-x}\right)$. U_1 and U_2 have been already used in (González-Hidalgo et al., 2009a). The rest of the considered uninorms belong to the class of $U_{\min}$. This class allows us to choose a uninorm with some desired underlying t-norm T and t-conorm S in the following way $U_{T,S,e}(x,y) =$

$$= \begin{cases} e \cdot T\left(\frac{x}{e},\frac{y}{e}\right) & \text{if } x,y \in [0,e], \\ e + (1-e) \cdot S\left(\frac{x-e}{1-e},\frac{y-e}{1-e}\right) & \text{if } x,y \in [e,1], \\ \min\{x,y\} & \text{otherwise.} \end{cases}$$

Thus we have considered U_3, U_4 and U_5 as the uninorms of the class of $U_{\min}$ given by

---

[1]Given a a conjunctive uninorm U, its RU-implication is defined by $I(x,y) = \sup\{t \in [0,1] | U(x,t) \leq y\}$.

Table 2: Considered implications.

Formula	Class
$I_1(x,y) = \begin{cases} \max\{1-x,y\} & \text{if } x \leq y, \\ \min\{1-x,y\} & \text{if } x > y. \end{cases}$	RU-implication
$I_2(x,y) = \begin{cases} \frac{(1-x)y}{x+y-2xy} & \text{if } (x,y) \notin \{(0,0),(1,1)\}, \\ 1 & \text{otherwise.} \end{cases}$	RU-implication
$I_3(x,y) = \begin{cases} \frac{1}{2}+y-x & \text{if } (y < x < \frac{1}{2}) \text{ or } (y > x \geq \frac{1}{2}), \\ \frac{1}{2} & \text{if } x \geq y \geq \frac{1}{2}, \\ 1 & \text{if } x \leq y < \frac{1}{2}, \\ y & \text{otherwise.} \end{cases}$	RU-implication
$I_4(x,y) = \begin{cases} 1 & \text{if } y = 1 \text{ or } x \leq y < \frac{1}{2}, \\ \max\{\frac{1}{2}-x,y\} & \text{if } y < x < \frac{1}{2}, \\ \frac{3}{2}-x & \text{if } \frac{1}{2} \leq x \leq y \text{ and } y > \frac{3}{2}-x, \\ \frac{1}{2} & \text{if } \frac{1}{2} \leq y < x, \\ y & \text{otherwise.} \end{cases}$	RU-implication
$I_5(x,y) = \begin{cases} y & \text{if } \frac{1}{2} \leq x < y, \\ \frac{1}{2} & \text{if } \frac{1}{2} \leq y \leq x, \\ 1 & \text{if } x \leq y < \frac{1}{2}, \\ y & \text{otherwise.} \end{cases}$	RU-implication
$I_6(x,y) = \begin{cases} 1 & \text{if } x = 0, \\ \frac{y^{2x}}{(1-y)^{2x}+y^{2x}} & \text{if } x > 0, y \leq \frac{1}{2} \\ \frac{y^{\frac{1}{2x}}}{(1-y)^{\frac{1}{2x}}+y^{\frac{1}{2x}}} & \text{otherwise.} \end{cases}$	(h,e)-implication
$I_7(x,y) = \begin{cases} \max\{\sqrt{1-x^2},y\} & \text{if } x \leq y, \\ \min\{\sqrt{1-x^2},y\} & \text{if } x > y. \end{cases}$	RU-implication

$U_{T_{LK},S_{LK},\frac{1}{2}}$, $U_{T_{nM},S_{nM},\frac{1}{2}}$ and $U_{T_M,S_M,\frac{1}{2}}$, respectively, where $T_{LK}(x,y) = \max\{x+y-1,0\}$, $T_M(x,y) = \min\{x,y\}$,

$$T_{nM}(x,y) = \begin{cases} 0 & \text{if } x+y \leq 1, \\ \min\{x,y\} & \text{otherwise,} \end{cases}$$

and S_{LK}, S_M and S_{nM} are their N_C-dual t-conorms, respectively (see (Klement et al., 2000) for more details). All the uninorms have neutral element $e = \frac{1}{2}$ except U_6, with neutral element $e = \frac{\sqrt{2}}{2}$.

On the other hand, we have considered 7 fuzzy implications. Six of them, from I_1 to I_5 and I_7, are in the same order the residual implications of the considered uninorms. Finally, I_6 is the (h,e)-implication generated by $h(x) = \ln\left(\frac{x}{1-x}\right)$. All these implications satisfy (NP$_e$) with $e = \frac{1}{2}$, except I_7 that satisfies it with $e = \frac{\sqrt{2}}{2}$. Thus 31 different configurations of uninorm and implications can be considered in the fuzzy gradient since U_6 and I_7 must be applied together.

3.1 NMS and Automatic Hysteresis

To compare the results, we need some objective performance measure on edge detection. These measures require, in addition to the binary edge image with edges of one pixel width (DE) obtained by the edge detector we want to evaluate, a reference edge image or *ground truth* edge image (GT) which is a binary edge image with edges of one pixel width containing the real edges of the original image. There are several measures of performance for edge detection in the literature, see (Papari and Petkov, 2011). In this paper we are going to use the measure proposed by Pratt, *Pratt's figure of merit*, to quantify the similarity between (DE) and (GT). This measure is defined by

$$FoM = \frac{1}{\max\{card\{DE\}, card\{GT\}\}} \cdot \sum_{x \in DE} \frac{1}{1+ad^2},$$

where *card* is the number of edge points of the image, *a* is a scaling constant and *d* is the separation distance of an actual edge point to the ideal edge points. In our case, we considered $a = 1$ and the Euclidean distance *d*. A higher value of *FoM* indicates a better capability to detect edges.

(a) Input original image.

(b) Fuzzy edge image obtained with the fuzzy gradient.

(c) NMS.

(d) Output binary thin edge image.
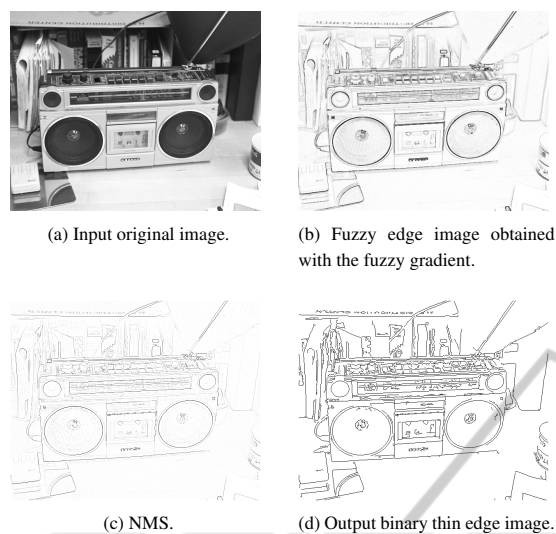
Figure 1: Sequence of the proposed algorithm.

However, the fuzzy based edge detectors generate an image where the value of a pixel represents its membership degree to the set of edges. This idea contradicts the restrictions of Canny (Canny, 1986), forcing a representation of the edges as binary images of one pixel width. Therefore the fuzzy edge image must be thinned and binarized. The fuzzy edge image will contain large values where there is a strong image gradient, but to identify edges the broad regions present in areas where the slope is large must be thinned so that only the magnitudes at those points which are local maxima remain. NMS performs this by suppressing all values along the line of the gradient that are not peak values (see (Canny, 1986)). NMS has been performed using P. Kovesis' implementation in Matlab (Kovesi, 2012).

Finally, to binarize the image, we have implemented an automatic, non-supervised, hysteresis based on the determination of the instability zone of the histogram to find the thresholds (see (Medina-Carnicer et al., 2011)). Hysteresis allows to choose which pixels are relevant in order to be selected as edges, using their membership values. Two threshold values T_1, T_2 with $T_1 \leq T_2$ are used. All the pixels with a membership value greater than T_2 are considered as edges, while those which are lower to T_1 are discarded. Those pixels whose membership value is between the two values are selected if and only if they are connected with other pixels above T_2. The method needs some initial set of candidates for the threshold values. In this case, $\{0.01, \ldots, 0.25\}$ has been introduced, the same set used in (Medina-Carnicer et al., 2011). In Figure 1, the sequence of the algorithm is displayed.

4 RESULTS AND ANALYSIS

The comparison method explained in the previous section needs an image database containing, in addition of the original images, their corresponding ground truth edge images in order to compare the outputs obtained by the different configurations. Thus, we have used the original images and their ground truth edge images of the public image database of the University of South Florida [2] (Bowyer et al., 1999). In this stage of our study, we have used 15 out of the 50 images of the database.

The results, obtained all of them using the following isotropic structuring element scaled by e, the neutral element of the uninorm,

$$B = e \cdot \begin{pmatrix} 0.86 & 0.86 & 0.86 \\ 0.86 & 1 & 0.86 \\ 0.86 & 0.86 & 0.86 \end{pmatrix}$$

which had been already used in (Nachtegael and Kerre, 2000), are summarized in Table 3. We have set the previous structuring element because it provides the best results with most of the configurations of the fuzzy gradient. However, we are aware that the results may differ if we change the structuring element. In the table, we compute some statistical measures associated to the obtained *FoM* values. For example, the mean value is the mean of the obtained *FoM* values using a particular configuration in the fuzzy gradient for the 15 considered images. As it can be observed, the most significant fact is the dependence of the election of the pair uninorm-implication into the results. Note that although some of the configurations obtain quite similar results, for example (U_4, I_1) and (U_4, I_6), the difference between the results obtained using the best configuration, that is (U_1, I_1), with respect to the worst one (U_3, I_3) is notable, a gap of 0.1644. The worst configuration according to its mean value is also the worst configuration for 12 of these images. On the other hand, the configuration with the highest mean value is not the configuration with the highest number of images for which a particular configuration is the best one of the 31 considered configurations, that is shared by (U_1, I_4) and (U_1, I_5). This is because the standard deviation of the *FoM* values obtained using (U_1, I_1) is lower than the one obtained using these two configurations, i.e., (U_1, I_1) is more stable. In Figure 2, we show some of the edge images obtained using some of these configurations. Note that the visual results agree with the *FoM* values since the results obtained by (U_3, I_3) contain, in general, few edges with respect to the others. Note that the presence of I_1 or

---

[2]It can be downloaded from ftp://figment.csee.usf.edu/ pub/ROC/edge_comparison_dataset.tar.gz

Table 3: Statistical measures associated to obtained *FoM* values.

Configuration		Mean	Std. Dev.	Images		Configuration		Mean	Std. Dev.	Images	
Unin.	Imp.			✓	×	Unin.	Imp.			✓	×
U_1	I_1	**0.4588**	0.0911	2	0	U_2	I_1	0.4406	0.0960	0	0
	I_2	0.4416	0.0883	0	0		I_2	0.4060	0.1088	1	0
	I_3	0.4295	0.0926	0	0		I_3	0.3953	0.1074	1	0
	I_4	0.4483	0.1004	**4**	0		I_4	0.4314	0.0947	1	0
	I_5	0.4482	0.1006	**4**	1		I_5	0.4317	0.0941	1	0
	I_6	0.4545	0.0925	3	0		I_6	0.4351	0.0854	1	0
U_3	I_1	0.4145	0.0849	0	0	U_4	I_1	0.4218	0.0787	0	0
	I_2	0.3682	0.1096	0	0		I_2	0.3807	0.1114	0	0
	I_3	0.2944	0.1127	1	12		I_3	0.3089	0.1206	0	1
	I_4	0.3584	0.0902	0	0		I_4	0.3645	0.0916	0	0
	I_5	0.3583	0.0903	0	0		I_5	0.3646	0.0916	0	0
	I_6	0.4146	0.0812	0	0		I_6	0.4218	0.0786	0	0
U_5	I_1	0.4218	0.0787	0	0	U_6	I_7	0.4417	0.0905	0	0
	I_2	0.3807	0.1114	0	0						
	I_3	0.3090	0.1207	0	1						
	I_4	0.3645	0.0916	0	0						
	I_5	0.3546	0.0916	0	0						
	I_6	0.4218	0.0786	0	0						

I_6 in a given configuration improves the results. Another fact to highlight is the similarity of the results obtained using U_4 and U_5 with a fixed implication. This is due to the similar expressions in a certain region of both uninorms and the choice of structuring element B. Finally, in Figure 3, the best configuration and the worst one for some images according to *FoM* are displayed.

To reinforce the previous analysis, a clustering method has been applied to study the relations between the configurations. Firstly, we have determined the optimal number of clusters according to the so-called F-test of variability reduction, leading to 4 clusters. Finally, applying the *K*-means algorithm with this number of clusters we have obtained the following results:

- Cluster 1: U_1 with $I_1 - I_6$, U_2 with I_1, $I_4 - I_6$, $U_3 - U_5$ with I_1 and I_6, U_6 with I_7.
- Cluster 2: U_2 with I_2 and I_3, $U_3 - U_5$ with I_2.
- Cluster 3: $U_3 - U_5$ with I_4 and I_5.
- Cluster 4: $U_3 - U_5$ with I_3.

These clusters allow us to set up a certain performance ranking with the considered logical operators:

$$U_1, U_6 \succ U_2 \succ U_3, U_4, U_5,$$
$$I_1, I_6, I_7 \succ I_2, I_4, I_5 \succ I_3,$$

where $A, B \succ C$ indicates that those configurations obtained from A or B give better results than those obtained from C.

From this ranking, some remarks can be stated:

1. Idempotent and representable uninorms generate better edge detectors than uninorms of the class $U_{\min}$.

2. The worst implication is I_3, that is the residual implication of the uninorm $U_{T_{LK},S_{LK},\frac{1}{2}}$. This fact is coherent with the bad behaviour of the Łukasiewicz t-norm in the morphology based on t-norms in $[0, 1]$.

3. The (h, e)-implication I_7 gives competitive results and therefore, the role of this class of implications in fuzzy morphology should be seriously investigated.

In Figure 4, these remarks can be graphically observed. In both subfigures, the vertical axis correspond to the mean of the *FoM* values of each configuration, while the horitzontal ones of Figure 4-(a) correspond to the different considered uninorms and analogously the different considered implications in Figure 4-(b). A dotted point is associated to the *FoM* value mean of a configuration (U_i, I_j).

5 CONCLUSIONS AND FUTURE WORK

In this work, a comparison of morphological gradients generated from different configurations of uninorm and fuzzy implication has been performed showing that the configuration (U_1, I_1) where U_1 is

(a) Original image.   (b) (U_1, I_1).   (c) (U_2, I_6).   (d) (U_3, I_3).
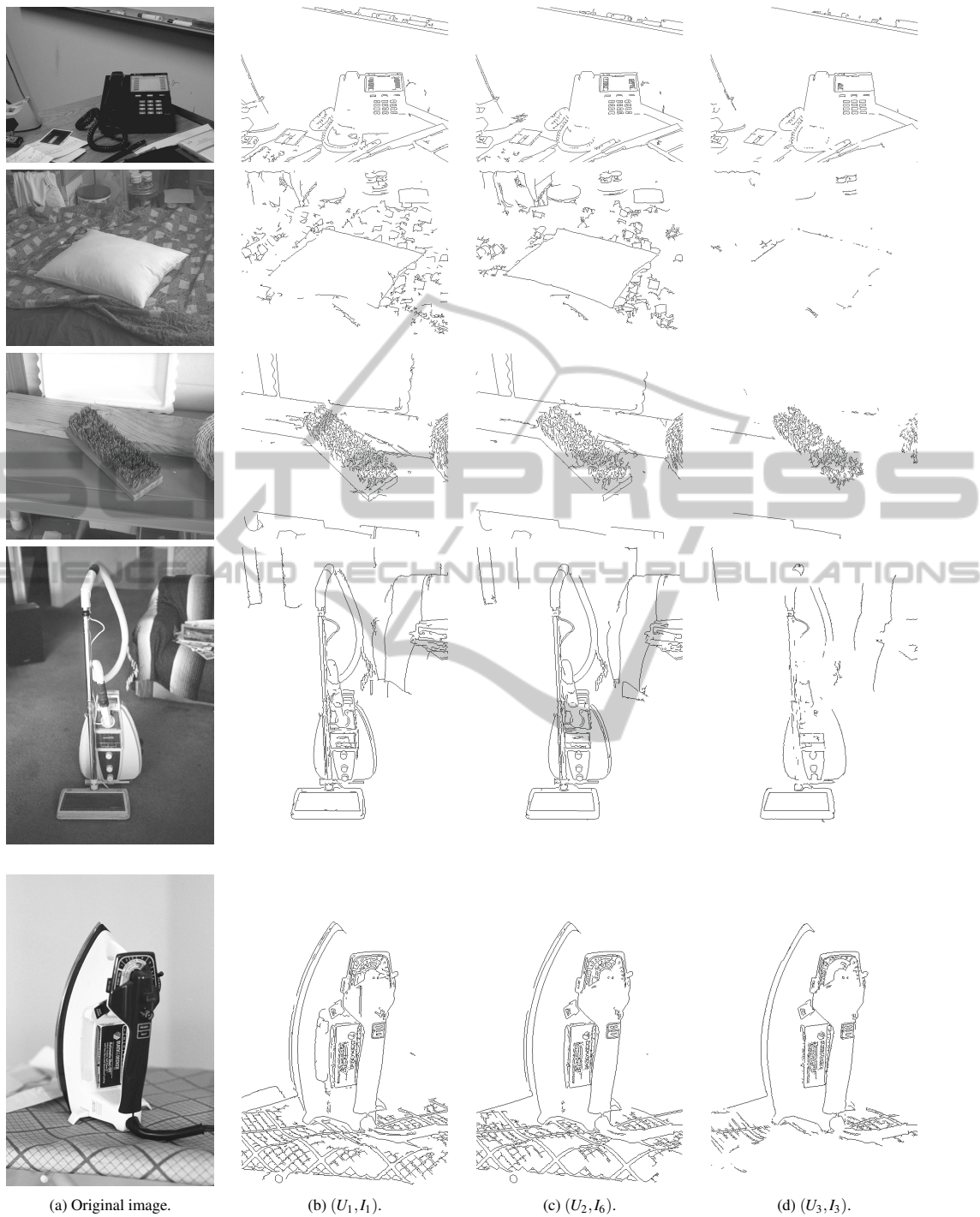
Figure 2: Some edge images obtained with different configurations.

the idempotent uninorm obtained from the classical negation and I_1 is its residual implication is the best configuration according to the performance measure on edge detection *FoM*. It has been shown that analogously to what happens on the morphology based on

t-norms, the uninorms generated in some region by the Łukasiewicz t-norm give bad results, both from the visual point of view and the *FoM* values obtained by the edge images. In addition, we have proved the possible use of the new class of implications, (h, e)-

(a) Original image.   (b) Ground truth.   (c) (U_1, I_4).   (d) (U_3, I_3).

(e) Original image.   (f) Ground truth.   (g) (U_1, I_6).   (h) (U_3, I_3).

(i) Original image.   (j) Ground truth.   (k) (U_1, I_4).   (l) (U_3, I_3).

(m) Original image.   (n) Ground truth.   (o) (U_1, I_1).   (p) (U_3, I_3).

(q) Original image.   (r) Ground truth.   (s) (U_2, I_4).   (t) (U_3, I_3).
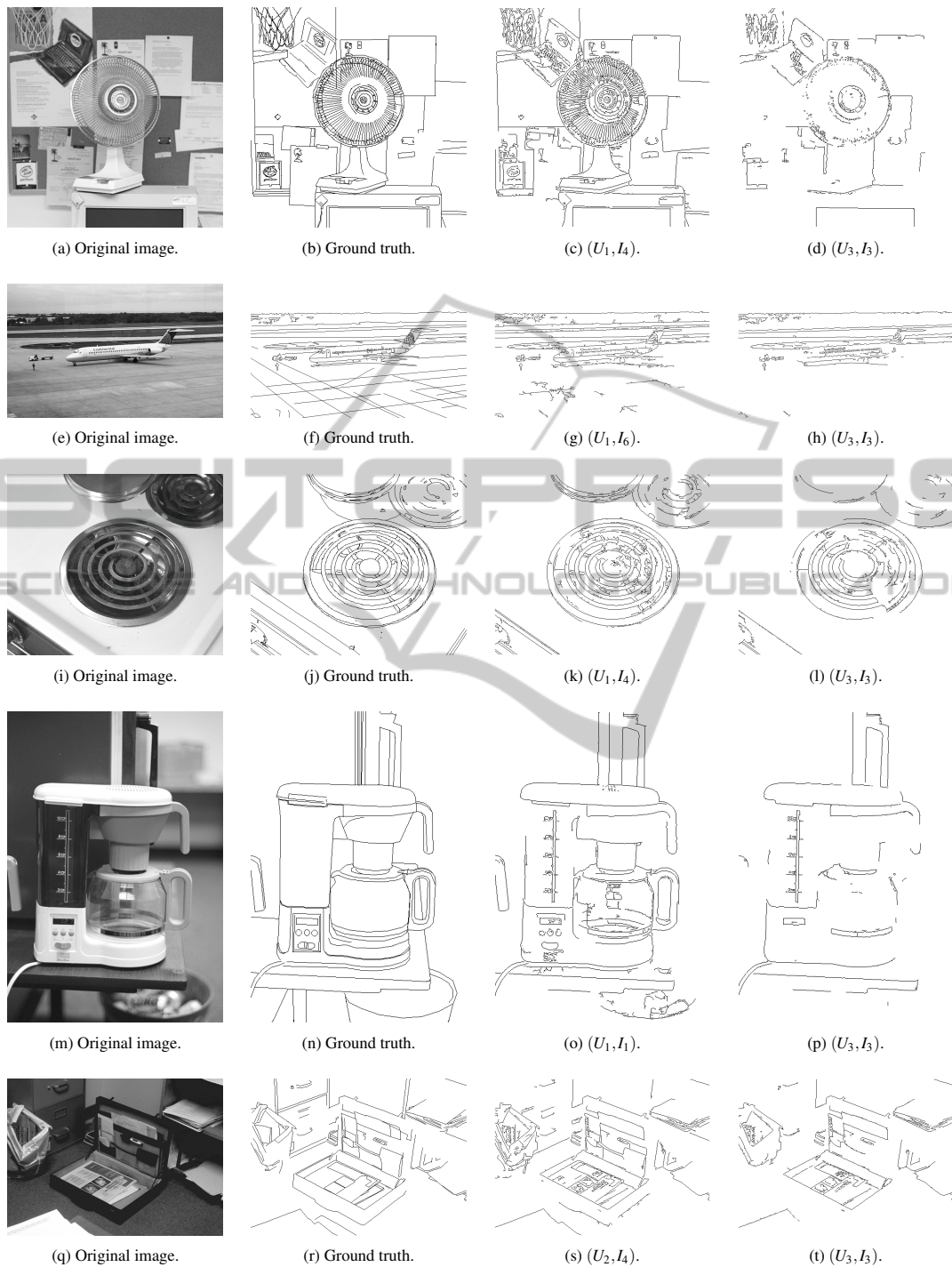
Figure 3: Best (3rd column) and worst (4th column) edge images obtained with the considered configurations according to their *FoM* value.

implications, in image processing applications.

In the future work, we want to to increase the number of images for the comparison including all the images in the used database. The next step would be the comparison of the uninorm edge detector generated by (U_1, I_1) with some classical edge detectors such as Canny, Sobel, Prewitt, etc. In addition, we want to generalize the morphological operators using a t-
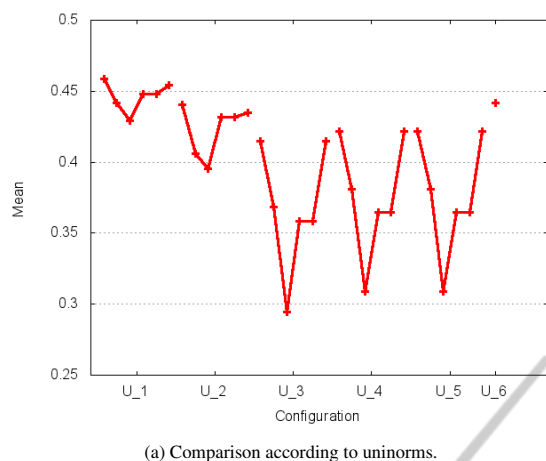
(a) Comparison according to uninorms.
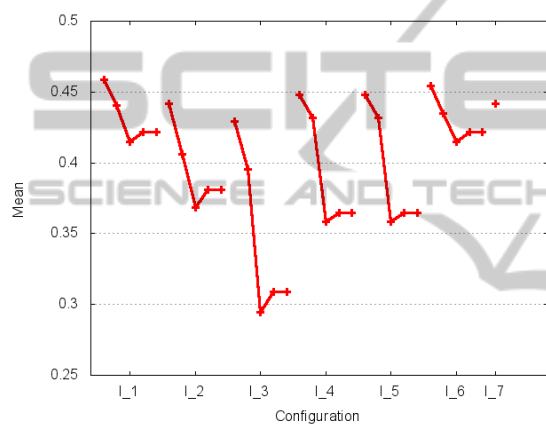
(b) Comparison according to implications.

Figure 4: Graphical comparison of the performance of the considered uninorms (a) and implications (b).

conorm and a t-norm rather than the operations sup and inf respectively in the dilation and erosion. As the maximum is the smallest of the t-conorms and the minimum is the largest of the t-norms, this generalization could improve the results since it would extend the morphological gradient allowing a greater detection of edges.

ACKNOWLEDGEMENTS

REFERENCES

Baczyński, M. and Jayaram, B. (2008). *Fuzzy Implications*, volume 231 of *Studies in Fuzziness and Soft Computing*. Springer, Berlin Heidelberg.

Bloch, I. and Maître, H. (1995). Fuzzy mathematical morphologies: a comparative study. *Pattern Recognition*, 28:1341–1387.

Bowyer, K., Kranenburg, C., and Dougherty, S. (1999). Edge detector evaluation using empirical ROC curves. *Computer Vision and Pattern Recognition*, 1:354–359.

Bustince, H., Barrenechea, E., Pagola, M., and Fernandez, J. (2009). Interval-valued fuzzy sets constructed from matrices: Application to edge detection. *Fuzzy Sets and Systems*, 160(13):1819–1840.

Canny, J. (1986). A computational approach to edge detection. *IEEE Trans. Pattern Anal. Mach. Intell.*, 8(6):679–698.

De Baets, B. (1997). Fuzzy morphology: A logical approach. In Ayyub, B. M. and Gupta, M. M., editors, *Uncertainty Analysis in Engineering and Science: Fuzzy Logic, Statistics, and Neural Network Approach*, pages 53–68. Kluwer Academic Publishers, Norwell.

De Baets, B. (2000). Generalized idempotence in fuzzy mathematical morphology. In Kerre, E. E. and Nachtegael, M., editors, *Fuzzy techniques in image processing*, number 52 in Studies in Fuzziness and Soft Computing, chapter 2, pages 58–75. Physica-Verlag, New York.

Fodor, J., Yager, R., and Rybalov, A. (1997). Structure of uninorms. *Int. J. Uncertainty, Fuzziness, Knowledge-Based Systems*, 5:411–427.

González-Hidalgo, M., Massanet, S., and J.Torrens (2010). Discrete t-norms in a fuzzy mathematical morphology: Algebraic properties and experimental results. In *Proceedings of WCCI-FUZZ-IEEE*, pages 1194–1201, Barcelona, Spain.

González-Hidalgo, M., Massanet, S., and Mir, A. (2012). Determining the best pair of t-norm and implication in the morphological gradient. In *Proceedings of XVI Congreso Español sobre Tecnologías y Lógica Fuzzy (ESTYLF)*, pages 510–515, Valladolid, Spain. (In Spanish).

González-Hidalgo, M., Mir-Torres, A., Ruiz-Aguilera, D., and Torrens, J. (2009a). Edge-images using a uninorm-based fuzzy mathematical morphology: Opening and closing. In Tavares, J. and Jorge, N., editors, *Advances in Computational Vision and Medical Image Processing*, number 13 in Computational Methods in Applied Sciences, chapter 8, pages 137–157. Springer, Netherlands.

González-Hidalgo, M., Mir-Torres, A., Ruiz-Aguilera, D., and Torrens, J. (2009b). Image analysis applications of morphological operators based on uninorms. In *Proceedings of the IFSA-EUSFLAT 2009 Conference*, pages 630–635, Lisbon, Portugal.

Klement, E., Mesiar, R., and Pap, E. (2000). *Triangular norms*. Kluwer Academic Publishers, London.

Kovesi, P. D. (2012). MATLAB and Octave functions for computer vision and image processing. Centre for Exploration Targeting, School of Earth and Environment, The University of Western Australia. Available from: http://www.csse.uwa.edu.au/~pk/research/matlabfns/.

Massanet, S. and Torrens, J. (2011). On a new class of fuzzy implications: h-implications and generalizations. *Information Sciences*, 181(11):2111 – 2127.

Medina-Carnicer, R., Muñoz-Salinas, R., Yeguas-Bolivar, E., and Diaz-Mas, L. (2011). A novel method to look for the hysteresis thresholds for the Canny edge detector. *Pattern Recognition*, 44(6):1201 – 1211.

Nachtegael, M. and Kerre, E. (2000). Classical and fuzzy approaches towards mathematical morphology. In Kerre, E. E. and Nachtegael, M., editors, *Fuzzy techniques in image processing*, number 52 in Studies in Fuzziness and Soft Computing, chapter 1, pages 3–57. Physica-Verlag, New York.

Papari, G. and Petkov, N. (2011). Edge and line oriented contour detection: State of the art. *Image and Vision Computing*, 29(2-3):79 – 103.

Pratt, W. K. (2007). *Digital Image Processing*. Wiley-Interscience, 4 edition.

Serra, J. (1982,1988). *Image analysis and mathematical morphology, vols. 1, 2*. Academic Press, London.